Complex Frequency versus Complex Propagation Constant Modeling and Q-Balancing in Periodic Structures

Simon Otto, Andreas Rennings, Klaus Solbach, and Christophe Caloz

University of Duisburg-Essen, Bismarckstr. 81, 47057 Duisburg, Germany
École Polytechnique de Montréal, 2500, ch. de Polytechnique, H3T 1J4, Montréal, Québec, Canada

***Abstract*—The paper compares the complex frequency modeling (eigenmode analysis) and the complex propagation constant modeling (drivenmode analysis) of periodic structures based on a generalized unit cell model, and derives the mathematical relation between these two approaches. Moreover, it shows that only under the condition of Q-balancing, the phase-frequency responses (dispersion diagrams) calculated by the two approaches are identical. The Q-balancing condition corresponds to the Heaviside condition for distortionless uniform lossy transmission lines, although it applies here to the different context of periodic structures. This study may provide deeper insight and understanding into the eigenmode analysis of periodic structures, which is commonly used by commercial simulators.**

***Index Terms*—complex frequency, complex propagation constant, distortionless propagation, drivenmode, eigenmode, Q-balancing, Heaviside condition, periodic structure.**

I. Introduction

The mathematical modeling of periodic structures dates back to the 19th century with the early derivations of Floquet [1], followed by the works of Brillouin [2] and Bloch [3], who dramatically advanced the electromagnetic theory of periodic structures and the quantum theory of solids, respectively, in the first part of the 20th century. Near the end of 20th century, periodic structures have known a regain of interest with photonic crystals [4], and this interest has been further boosted with the advent of metamaterials [5], [6], [7] at the turn of the 21st century. The numerous applications of periodic structures, for instance in traveling-wave amplifiers and antenna arrays, along with the development of novel periodic systems, represent a strong motivation for further research on the subject.

One of the most significant advances in modern periodic structures has been the fundamental concept of composite right/left-handed (CRLH) artificial structures [5]. Such structures can be designed to exhibit a closed electromagnetic band gap between the left-handed (backward) and right-handed (forward) frequency ranges for a seamless transition across a *zero-phase transition frequency*, where the phase of the fundamental space harmonic vanishes. The corresponding condition is generally referred to as the *frequency-balancing condition*, which requires that the series and shunt resonances of the structure be tuned to the same frequency for pole-zero cancellation. In [8], it has been demonstrated that a broad class of periodic structures can be modeled and understood within the CRLH framework, with immediate application to periodic leaky-wave antennas, and a generalized transmission line (TL) equivalent model has been established to extend CRLH TL analysis.

At the zero-phase frequency, the wave propagation is dominated by resistive contributions, which strongly affect the group velocity, causing the conventional perturbation approach to fail. Despite its simplicity, the generalized TL equivalent model, with its four equivalent LCRG constitutive parameters, has proven successful in the modeling wave propagation around this transition point [8]. Moreover, [8] and [9] have established a novel *Q-balancing condition*, which ensures distortionless periodic response under equal quality factors of the series and shunt resonators, using a *complex propagation constant* modeling approach in the generalized TL model and in the particular CRLH TL model [5], respectively. Q-balancing, which is similar to the Heaviside condition for distortionless *uniform* lossy transmission lines [10], essentially balances the resistive and the reactive contributions in the unit cell, yielding distortionless propagation (constant group delay), thereby overcoming the issue of strong dispersive effects due to loss across the transition frequency (corresponding to angle-dependent maximal gain in a leaky-wave antenna).

This paper compares the *complex propagation constant* approach (driven mode analysis) and the *complex frequency* approach (eigenmode analysis) to determine the dispersion diagram of a periodic structure, using generalized TL modeling. It derives the mathematical relation linking the two approaches, interprets dispersion for lossy periodic structures, and confirms the Q-balancing condition, consistently with the two approaches.

II. Network Modeling

In the forthcoming derivations, the following restrictions are imposed on the unit cell under consideration: 1) it is transversally symmetrical, i.e. its axial impedance parameters are equal: $Z_{11} = Z_{22}$, 2) it is frequency balanced, and 3) it has a quasi-linear dispersion characteristic near the zero-phase frequency. Figures 1(a) and (b) illustrate the complex frequency and complex propagation constant approaches, respectively.

A. Complex Propagation Constant - Drivenmode Analysis

Figure 2(a) shows the unit cell model for the complex propagation constant approach. In this section, we briefly recall the TL modeling presented in [8]. We assume frequency balancing, i.e. $\omega_{se} = \omega_{sh} = \omega_0$, where the subscripts *se*, *sh* and 0 refer to series, shunt, and to transition frequencies,

978-1-4673-1088-8/12/$31.00 ©2012 IEEE

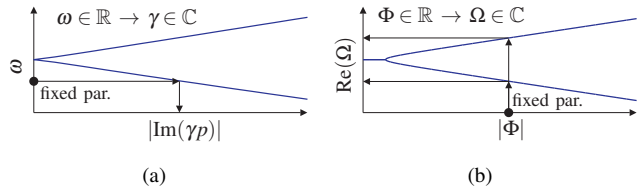

(a) (b)

Fig. 1. Two approaches considered to determine the dispersion diagram of a periodic structure. (a) Complex propagation constant approach: a real frequency ω is fixed, and the corresponding complex propagation constant γ is computed. (b) Complex frequency approach: a real unit cell phase shift Φ is fixed, and the corresponding complex frequency Ω is computed.

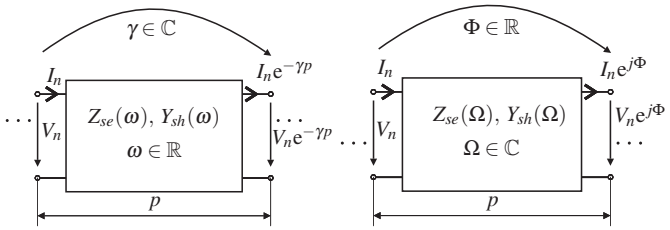

(a) (b)

Fig. 2. Unit cell modeling and parameter definitions for (a) the complex propagation approach [Fig. 1(a)], and (b) the complex frequency approach [Fig. 1(b)].

respectively [5]. Consider the frequency ω, deviating by $\Delta\omega$ from the transition frequency ω_0, i.e. $\omega = \omega_0 + \Delta\omega$. The immittances of the series and the shunt resonators under linearized reactance $2\Delta\omega L$ and susceptance $2\Delta\omega C$ slopes read

$$Z_{se}(\Delta\omega) = R + j2\Delta\omega L = R\left(1 + j\frac{2\Delta\omega}{\omega_0}Q_{se}\right), \tag{1a}$$

$$Y_{sh}(\Delta\omega) = G + j2\Delta\omega C = G\left(1 + j\frac{2\Delta\omega}{\omega_0}Q_{sh}\right), \tag{1b}$$

where $Q_{se} = \omega_0 L/R$ and $Q_{sh} = \omega_0 C/G$ are the series and shunt quality factors, respectively. The parameters R and G model the series and shunt losses, respectively, and they are assumed constant. Using a homogenization procedure for the limit $|\gamma| \rightarrow 0$, the complex propagation constant might be approximated as

$$\gamma = \alpha + j\beta = \frac{\sqrt{Z_{se}(\Delta\omega)Y_{sh}(\Delta\omega)}}{p}. \tag{2}$$

Asymptotic formulas near the transition frequency ($\Delta\omega \approx 0 \rightarrow$ subscript 0) and off-transition frequencies ($|\Delta\omega| \gg 0 \rightarrow$ subscript Δ) have been subsequently derived in [8]:

$$\alpha_0 p = \sqrt{RG}, \quad \beta_0 p = \frac{\Delta\omega}{\omega_0}\sqrt{RG}\,(Q_{se} + Q_{sh}), \tag{3}$$

$$\alpha_\Delta p = \frac{1}{2}\omega_0\sqrt{LC}\left(\frac{1}{Q_{se}} + \frac{1}{Q_{sh}}\right), \quad \beta_\Delta p = 2\Delta\omega\sqrt{LC}. \tag{4}$$

Under the Q-balancing condition, $Q_{se} = Q_{sh} = Q_{bal}$, (2) simplifies to $\gamma p = \sqrt{RG}(1 + j2\Delta\omega/\omega_0 Q_{bal}) = \sqrt{RG} + j2\Delta\omega\sqrt{LC}$, where the loss and propagation terms are clearly decoupled, and where it appears that the 0 and Δ regimes yield the same propagation parameters: $\alpha_0 = \alpha_\Delta = \alpha_{bal}$ and $\beta_0 = \beta_\Delta = \beta_{bal}$.

B. Complex Frequency Modeling - Eigenmode Analysis

Figure 2(b) shows the unit cell model for the complex frequency modeling approach. Consider the complex frequency $\Omega = \Omega_{re} + j\Omega_{im} = \Omega_0 + \Delta\Omega_{re} + j\Omega_{im} = \Omega_0 + \Delta\Omega$, with the complex frequency deviation $\Delta\Omega = \Delta\Omega_{re} + j\Omega_{im}$ from Ω_0. Substituting $\Delta\omega$ by $\Delta\Omega$ in (1) yields

$$Z_{se}(\Delta\Omega) = R + j2L\Delta\Omega = R\left(1 + j\frac{2\Delta\Omega}{\Omega_0}Q_{se}\right), \tag{5a}$$

$$Y_{sh}(\Delta\Omega) = G + j2C\Delta\Omega = G\left(1 + j\frac{2\Delta\Omega}{\Omega_0}Q_{sh}\right). \tag{5b}$$

The dispersion relation corresponding to (2) reads then

$$j\Phi = \sqrt{Z_{se}(\Delta\Omega)Y_{sh}(\Delta\Omega)}, \tag{6}$$

where Φ is the phase (real quantity) across the unit cell, as shown in Fig. 2(b). Inserting (5) into (6), and solving the resulting equation for $\Delta\Omega$, we get

$$\Delta\Omega = \frac{1}{2\sqrt{LC}} \cdot \left(\pm\sqrt{\Phi^2 + \frac{RG}{2} - \frac{(LG)^2 + (CR)^2}{4LC}} + j\frac{LG + CR}{2\sqrt{LC}}\right) \tag{7}$$

After some algebraic manipulations, (7) may be written in terms of the asymptotic propagation constants by replacing the LCRG expression in (7) using (3) and (4):

$$\Delta\Omega = \frac{1}{\left.\dfrac{\partial\beta_\Delta p}{\partial\omega}\right|_{\omega_\Delta}}\left(\pm\sqrt{\Phi^2 + (\alpha_0 p)^2 - (\alpha_\Delta p)^2} + j\alpha_\Delta p\right). \tag{8}$$

Equation (8) links the two modeling approaches and forms the central result of the paper. Due to the fundamental importance of this result, we shall further investigate and interpret it in the remainder of the paper. For small Φ, $\Phi^2 + (\alpha_0 p)^2 - (\alpha_\Delta p)^2 < 0$, and the square root only contributes to imaginary frequencies resulting in $\mathrm{Re}(\Delta\Omega) = 0$. In contrast, for large Φ, $\Phi^2 + (\alpha_0 p)^2 - (\alpha_\Delta p)^2 > 0$, the square root only contributes to the real part of the complex frequency. We may now define the transition phase Φ_{tr} as the phase where the radicand changes sign, i.e. $\Phi_{tr}^2 + (\alpha_0 p)^2 - (\alpha_\Delta p)^2 = 0$:

$$\Phi_{tr} = \pm\sqrt{(\alpha_\Delta p)^2 - (\alpha_0 p)^2}. \tag{9}$$

III. Comparison Results

This section compares dispersion curves obtain from the two approaches described in Sec. II.

A. Q-Unbalanced Case

Figure 3 illustrates the Q-balanced case, with $Q_{se} = 10$ and $Q_{sh} = 200$, obtained from the set of parameters: $L = 4$ nH, $C = 0.1$ pF, $R = 60.32\ \Omega$, $G = 75.4\ \mu$S, and $\Omega_0 = 24$ GHz. The left axis pertains to the real frequency $\mathrm{Re}(\Omega) = \Omega_{re}$ as well as ω, while the right axis pertains to the imaginary frequency with $\mathrm{Im}(\Omega) = \Omega_{im}$. The transition phase Φ_{tr} is clearly

978-1-4673-1088-8/12/$31.00 ©2012 IEEE

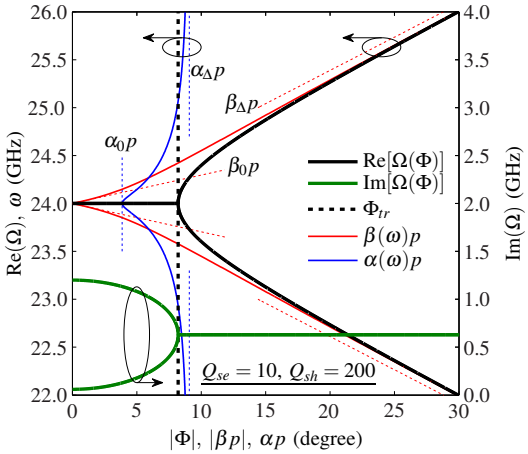

Fig. 3. Dispersion diagram comparing the complex frequency and complex propagation constant curves for the Q-unbalanced case with $Q_{se} = 10$ and $Q_{sh} = 200$. The Φ and βp curves are very different around the transition phase $\Phi_{tr} = 8.3°$.

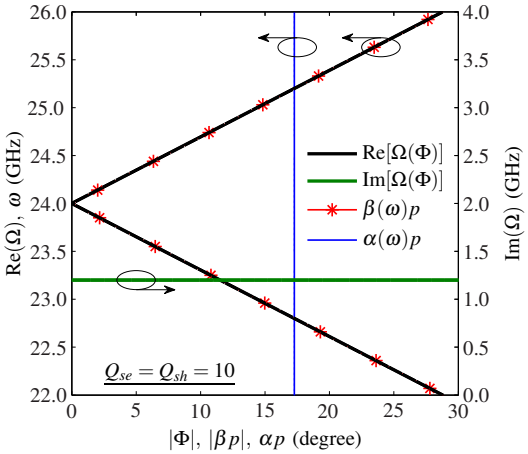

Fig. 4. Dispersion diagram comparing the complex frequency and complex propagation constant curves for the Q-balanced case with $Q_{se} = 10$ and $Q_{sh} = 10$. The $\Phi = \beta p$ curves are superimposed.

identified at the separation of the *constant* and Φ-*dependent* regimes for both real and imaginary frequencies, which shows the predicted complementary behavior. The deviation between the two approaches is clearly maximal at this transition phase, Φ_{tr}, and decreases progressively as Φ or βp increase, where the modeling approaches converge to the same frequency: $\Omega_{re} \leftrightarrow \omega$.

B. Q-Balanced Case

We now investigate the Q-balanced case, with the design $Q_{se} = Q_{sh} = 10$, obtained by increasing the shunt loss to $G = 1.51$ mS. The results are plotted in Fig. 4. As predicted and shown in [8], α is now constant versus frequency, and $\alpha_0 = \alpha_\Delta = \alpha_{bal}$, from which, using (9), $\Phi_{tr} = 0$. Furthermore, (8) simplifies to

$$\Delta\Omega = \frac{1}{\dfrac{\partial \beta_{bal} p}{\partial \omega}} \left(\pm|\Phi| + j\alpha_{bal} p\right) = \frac{v_g}{p}\left(\pm|\Phi| + j\alpha_{bal} p\right), \quad (10)$$

where v_g denotes the group velocity. Multiplying (10) by the group delay through a unit cell, $\tau_g = p/v_g$ [11], we get

$$\Delta\Omega\tau_g = \Delta\Omega_{re}\tau_g + j\Omega_{im}\tau_g = \pm|\Phi| + j\alpha_\Delta p. \quad (11)$$

This complex frequency result may be compared with its complex propagation constant counterpart,

$$\beta p = 2\Delta\omega\sqrt{LC} = \Delta\omega\frac{p}{v_g} = \Delta\omega\tau_g. \quad (12)$$

Substituting $\Delta\omega = \Delta\Omega_{re}$ in this equation, we find, by comparison with (11), that $|\beta p| = |\Phi|$, as shown in Fig. 4, indicating that the functions Φ and βp are both *dispersionless* (linear functions of the frequency) and *identical* under Q-balancing. In contrast, the Im(Ω) and αp curves are perpendicular to each other.

IV. Conclusion

We have compared the complex frequency modeling (eigenmode analysis) and the complex propagation constant modeling (drivenmode analysis) of periodic structures based on a generalized unit cell model, and derived the mathematical relation between these two approaches. Moreover, we have shown that the real frequency response of the former approach and the phase frequency response of the latter approach are generally different, but identical and dispersionless under the Q-balancing condition, which is identical to the Heaviside condition for dispersionless uniform lossy transmission lines, although it applies here to the different context of periodic structures.

References

[1] G. Floquet, "Sur les équations différentielles linéaires à coefficients périodiques," *Annales École Normale Supérieure*, vol. 12, pp. 47–88, 1883.

[2] L. Brillouin, *Wave Propagation in Periodic Structures*. Dover Publications Inc., 1946.

[3] F. Bloch, "Über die Quantenmechanik der Elektronen in Kristallgittern," *Z. Physik*, vol. 52, pp. 555–600, 1928.

[4] J. D. Joannopoulos, S. G. Johnson, J. N. Winn, and R. D. Meade, *Photonic Crystals: Molding the Flow of Light (Second Edition)*. Princeton University Press, 2008.

[5] C. Caloz and T. Itoh, *Electromagnetic Metamaterials: Transmission Line Theory and Microwave Applications*. Wiley-IEEE Press, 2005.

[6] G. V. Eleftheriades and K. G. Balmain, *Negative Refraction Metamaterials: Fundamental Principles and Applications*. Wiley-IEEE Press, 2005.

[7] N. Engheta and R. W. Ziolkowski, *Electromagnetic Metamaterials: Physics and Engineering Explorations*, N. Engheta and R. W. Ziolkowski, Eds. Wiley-IEEE Press, 2006.

[8] S. Otto, A. Rennings, K. Solbach, and C. Caloz, "Transmission line modeling and asymptotic formulas for periodic leaky-wave antennas scanning through broadside," *IEEE Trans. Antennas Propag.*, vol. 59, no. 10, October 2011.

[9] J. S. Gomez-Diaz, D. Cañete Rebenaque, and A. Alvarez-Melcon, "A simple CRLH LWA circuit condition for constant radiation rate," *IEEE Antennas Wireless Propag. Lett.*, vol. 10, pp. 29–32, 2011.

[10] O. Heaviside, "Electromagnetic induction and its propagation," *The Electrician,*, vol. August 7, pp. pp. 230–231, 1887.

[11] R. E. Collin, *Foundations for Microwave Engineering*. Wiley-IEEE Press, December 2000.

978-1-4673-1088-8/12/$31.00 ©2012 IEEE